ARTICLE

OBC
www.rsc.org/obc

A new kinetic approach to the evaluation of rate constants for the spin trapping of superoxide/hydroperoxyl radical by nitrones in aqueous media

Robert Lauricella, Ahmad Allouch, Valérie Roubaud, Jean-Claude Bouteiller and Béatrice Tuccio *

Laboratoire TRACES, Case 541, Université de Provence, Faculté de Saint Jérôme, Av. Escadrille Normandie Niemen, 13397 Marseille Cedex 20, France

Received 28th January 2004, Accepted 5th March 2004
First published as an Advance Article on the web 29th March 2004

A new kinetic approach to the evaluation of rate constants for the spin trapping of superoxide/hydroperoxyl radical by nitrones in buffered media is described. This method is based on a competition between the superoxide trapping by the nitrone and the spontaneous dismutation of this radical in aqueous media. EPR spectra are recorded as a function of time at various nitrone concentrations, and kinetic curves are obtained after treatment of these spectra using both singular value decomposition and pseudo-inverse deconvolution methods. Modelling these curves permits the determination of the rate constants k_T and k_D for the superoxide trapping and the adduct decay reactions, respectively. Kinetics parameters thus obtained with six nitrones, namely the 2-ethoxycarbonyl-2-methyl-3,4-dihydro-2*H*-pyrrole *N*-oxide (EMPO) **1**, the 5-diethoxyphosphoryl-5-methyl-3,4-dihydro-5*H*-pyrrole *N*-oxide (DEPMPO) **2**, the 5,5-dimethyl-3,4-dihydro-5*H*-pyrrole *N*-oxide (DMPO) **3**, the 1,3,5-tri[(*N*-(1-diethylphosphono)-1-methylethyl)-*N*-oxy-aldimine]benzene (TN) **4**, the *N*-benzylidene-1-ethoxycarbonyl-1-methylethylamine *N*-oxide (EPPN) **5**, and the *N*-[(1-oxidopyridin-1-ium-4-yl)methylidene]-1-ethoxycarbonyl-1-methylethylamine *N*-oxide (EPPyON) **6**, indicate that cyclic nitrones trapped superoxide faster than the linear ones. However, the low k_T values obtained for compounds **1**–**6** show that there is still a need for new molecules with better spin trapping capacities.

Introduction

The observation that superoxide could play an important role in initiating oxidative damage in biological systems generated a considerable increase in the development of more sensitive probes to detect this radical in biological milieu.[1] In this field, the EPR-spin trapping technique using nitrones has received particular attention.[2] Among all the conditions that a nitrone must fulfil to be considered as an efficient superoxide detector, kinetic criteria are of crucial importance: a nitrone must trap rapidly superoxide, leading to a long-lived spin adduct. It is now quite easy to determine the decay rate of nitrone superoxide adducts,[3–10] while it is much more difficult to perform kinetic studies of the trapping reaction. This is the reason why, until recently, only a few papers have reported rate constants for the superoxide spin trapping.[11–13] Most of them have been obtained using the kinetic competition method with superoxide scavengers, which suffers from serious disadvantages. First, it does not permit the absolute value of the trapping rate constant to be obtained directly. In this method, there is also an uncertainty associated with the assumed values of some rate constants. Thus, a survey of the literature data shows a discrepancy between the rate constant values given for the reaction of superoxide with ferricytochrome c, frequently used to calibrate the superoxide source, and this yielded an uncertainty in the determination of the trapping kinetic data.[11c,14] Neglecting both the superoxide dismutation and the decay of the resultant spin adduct can also be a significant source of error. Last, all the calculations are based on initial rates of the adduct formation, which determination often lacks precision. The recent publication of three new papers dealing with the superoxide trapping kinetics shows a renewal of interest in this topic.[10,15,16] The important discrepancy between the results given in these papers is noteworthy, and could originate both in the use of initial rates in the calculations and in the calibration of the superoxide source using cytochrome c. There is obviously a need for an efficacious and reliable method to study the superoxide trapping kinetics.

In this paper, we propose a new kinetic approach to the evaluation of rate constants for the spin trapping of superoxide radical by nitrones, and we describe its application to the case of six nitrones, namely the 2-ethoxycarbonyl-2-methyl-3,4-dihydro-2*H*-pyrrole *N*-oxide (EMPO) **1**, the 5-diethoxyphosphoryl-5-methyl-3,4-dihydro-5*H*-pyrrole *N*-oxide (DEPMPO) **2**, the 5,5-dimethyl-3,4-dihydro-5*H*-pyrrole *N*-oxide (DMPO) **3**, the 1,3,5-tri[(*N*-(1-diethylphosphono)-1-methylethyl)-*N*-oxy-aldimine]benzene (TN) **4**, the *N*-benzylidene-1-ethoxycarbonyl-1-methylethylamine *N*-oxide (EPPN) **5**, and the *N*-[(1-oxidopyridin-1-ium-4-yl)methylidene]-1-ethoxycarbonyl-1-methylethylamine *N*-oxide (EPPyON) **6** (Scheme 1).

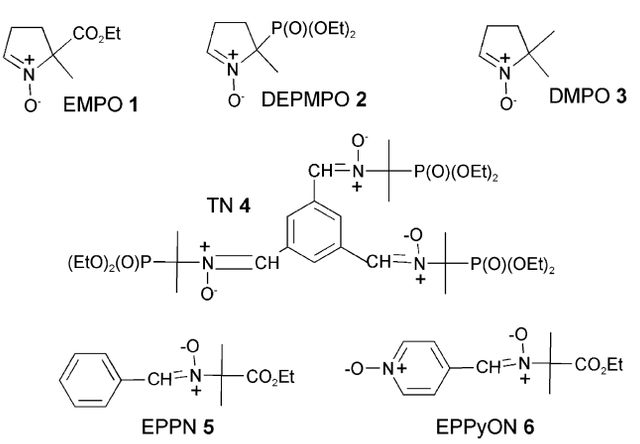

Scheme 1 Formulae of the nitrone spin traps studied.

Results and discussion

Presentation of the method

The rate constant values determined for the trapping reaction are pH dependent and include the contribution of both $O_2^{-\bullet}$

DOI: 10.1039/b401333f

and $HO_2^{\bullet}$ trapping. The term "superoxide" will frequently be used instead of "superoxide and hydroperoxyl radicals" throughout this text, with the aim of shortening the notations. The basic principle of this method involves a competition between the spin trapping of superoxide by the nitrone and the spontaneous dismutation of this radical in aqueous media. When compared to the use of competitive superoxide scavengers, this approach presents the important advantage of being more easily implemented. It does not require the preliminary determination of the rate constant for the reaction of superoxide with the scavenger, the medium does not contain a scavenger that could initiate side reactions, and the rate constant for the superoxide spontaneous dismutation has been previously determined in a wide pH range.[17] In addition, our method permits the consideration of the whole kinetic curve of superoxide spin adduct formation and decay, which avoids errors due to the determination of initial rates. Then, the effect of varying the nitrone concentration on the spin trapping rate is examined, and all the kinetic curves obtained are modelled simultaneously with the help of the home-made computer program KALIDAPHNIS, as described in the Experimental section. It should be noted that our method only refers to the superoxide spontaneous dismutation and does not necessitate the calibration of the superoxide source.

The xanthine/xanthine oxidase (X/XO) system was used to generate superoxide in phosphate buffers in the presence of the nitrone N. The superoxide produced can decay either by reaction with N, giving rise to the superoxide adduct N–O_2H, or by spontaneous dismutation. Let k_T and k_{dis} be the second order rate constants of the trapping and the dismutation reactions, respectively. When the nitrone concentration is sufficiently high to trap out most of the superoxide produced, the spontaneous dismutation becomes negligible. Under these conditions, the rate of N–O_2H formation does not depend on the value of k_T, and corresponds to the rate of superoxide production. Thus, the experimental curve representing the variation of N–O_2H concentration with time depends only on the rates of superoxide production (eqn. (1)) and of spin adduct decay (eqn. (4)). On the basis of the various examples studied, we have found that a simple overall first-order process permitted to correctly model the production of superoxide, according to eqn. (1), in which X is an intermediate derived from xanthine, and k_X a first-order rate constant. It is important to specify that our purpose was just to model the appearance of superoxide in the medium. It is obvious that the mechanism responsible for the superoxide production by the X/XO system could be more complex than a first-order process. At lower N concentration, a competition between the trapping and the dismutation reactions occurs. The corresponding kinetic model can be described by reactions (1)–(4) (see Scheme 2), in which k_D is the rate constant for the pseudo-first order decay of N–O_2H, Y representing EPR-silent products. In a first approximation, an eventual second order decay of N–O_2H, due to a disproportionation reaction of this radical, was neglected. The rate equations (5)–(8) given in Scheme 3 can be written from these reactions.

$$X \xrightarrow{k_X} O_2^{\bullet-} \quad (1)$$

$$2\,O_2^{\bullet-} + 2\,H^+ \xrightarrow{k_{dis}} O_2 + H_2O_2 \quad (2)$$

$$O_2^{\bullet-} + N + H^+ \xrightarrow{k_T} N\text{-}O_2H \quad (3)$$

$$N\text{-}O_2H \xrightarrow{k_D} Y \quad (4)$$

Scheme 2 Reactions (1)–(4) considered in the kinetic model.

To sum up, the following procedure was used to evaluate k_T. In a first step, three series of EPR spectra were recorded at three nitrone concentrations in the presence of an internal reference.

$$\frac{d[X]}{dt} = -k_X [X] \quad (5)$$

$$\frac{d[O_2^{\bullet-}]}{dt} = k_X [X] - k_T [N] [O_2^{\bullet-}] - 2\,k_{dis} [O_2^{\bullet-}]^2 \quad (6)$$

$$\frac{d[N\text{-}O_2H]}{dt} = k_T [N] [O_2^{\bullet-}] - k_D [N\text{-}O_2H] \quad (7)$$

$$\frac{d[N]}{dt} = -k_T [N] [O_2^{\bullet-}] \quad (8)$$

Scheme 3 Rate equations (5)–(8) considered in the kinetic model.

The singular value decomposition (SVD) method was applied to reduce the noise, and the kinetic curves, representing N–O_2H concentration *vs.* time, were obtained after deconvolution of the signal using the pseudo-inverse procedure (see Experimental section). Note that the parameters X_i and k_X are characteristic of the solutions used to produce superoxide. Consequently, these experiments must be done with the same superoxide generator exactly, in order to avoid a variation of the superoxide production rate. In a second step, the experimental kinetic curves were modelled by computer integration of equations (5)–(8). In these calculations, the k_{dis} value was obtained from literature,[17a] initial concentrations of N–O_2H and $O_2^{\bullet-}$ were equal to zero, while initial concentration of nitrone was an experimental parameter. Using the least squares method, the other parameters (X_i initial concentration of X, k_X, k_T and k_D) were determined by fitting the calculated curve to the experimental one. The curves obtained at the various nitrone concentrations were considered jointly, and modelled with the same parameter set (X_i, k_X, k_T), except for those which varied with the nitrone concentration (initial concentration of nitrone and k_D).

Application to the determination of superoxide trapping rate by nitrones

All the nitrones considered in our study have been successfully used in the past to trap superoxide in neutral media.[3–6,9,11,13] In order to explain more clearly our method, we have chosen to detail its application to the determination of the rate constant for the trapping of superoxide by EMPO **1** at pH 7.2. At this pH, k_{dis} is equal to 4.03 10^5 dm^3 mol^{-1} s^{-1}.[17a] Three experiments were performed by generating superoxide in the presence of 10 mmol dm^{-3}, 30 mmol dm^{-3}, and 200 mmol dm^{-3} EMPO, respectively, and of 3-carboxy-2,2,5,5-tetramethylpyrrolidin-1-oxyl (3CP), used as internal reference. A standard spectrum recorded under these conditions, showing the presence of 3-CP stable radical and of the superoxide spin adduct EMPO–O_2H, has been reproduced in Fig. 1.

A part of this EPR spectrum (framed portion in Fig. 1) was then recorded every 42 s. Fig. 2 shows on the left five spectra recorded under these conditions at different times using 10 mmol dm^{-3} EMPO, and on the right the same spectra obtained after noise-reduction by the SVD procedure.

The kinetic curves (EMPO–O_2H concentration *vs.* time) obtained after deconvolution of experimental signals are given in Fig. 3. An attempt to model the curve obtained at low nitrone concentration alone using equations (5)–(8) (10 mmol dm^{-3}, Fig. 3, trace a) indicated that too many unknown parameters had to be determined from a single curve, and yielded meaningless results. On the other hand, modelling the curve recorded at high nitrone concentration solely (200 mmol dm^{-3}, Fig. 3, trace c) showed that all superoxide produced was trapped by the nitrone, and the values of the rate constants k_{dis} and k_T had no influence on the curve calculated. Consequently, the shape of the curve obtained at high nitrone concentration depended only on the rates of superoxide production and of EMPO–O_2H decay, and its simulation led to an accurate evaluation of X_i, k_X, and k_D. Considering and modelling the three experimental

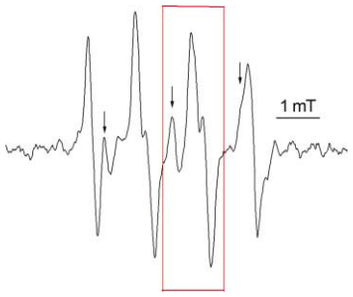

Fig. 1 EPR signal obtained in a pH 7.2 buffer by generating superoxide with a xanthine/xanthine oxidase system in the presence of 0.01 mol dm^{-3} EMPO and of 0.6 10^{-6} mol dm^{-3} 3CP. The main signal corresponds to the EPR spectrum of EMPO–O_2H. The three lines of the 3CP spectrum are marked by downward arrows. The framed part corresponds to the portion of the signal chosen to perform the kinetic experiments (see Fig. 2). The instrument settings were as follows: microwave power, 20 mW; scan time, 21 s; time constant, 164 ms; receiver gain, 1.26×10^6; modulation amplitude, 0.15 mT; 2 scans.

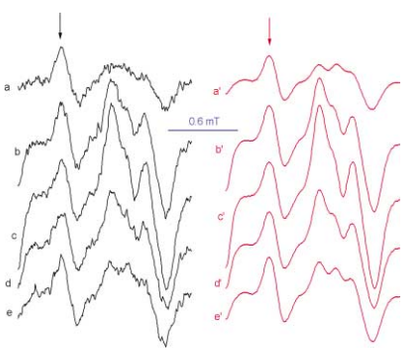

Fig. 2 **a–e** (in black): EPR spectra obtained by generating superoxide in the presence of 0.01 mol dm^{-3} EMPO and of 0.6 10^{-6} mol dm^{-3} 3CP, and recorded 42 s (a), 3 min 30 s (b), 14 min (c), 28 min (d) and 56 min (e) after the beginning of the trapping reaction, **a′-e′** (in red): the same signals after application of the SVD procedure. The spectra correspond to the framed part of the signal reproduced in Fig. 1. The line marked by a downward arrow belongs to 3CP. The instrument settings were as follows: microwave power, 20 mW; scan time, 21 s; time constant, 164 ms; receiver gain, 10^6; modulation amplitude, 0.15 mT; 2 scans, scan width, 1.5 mT.

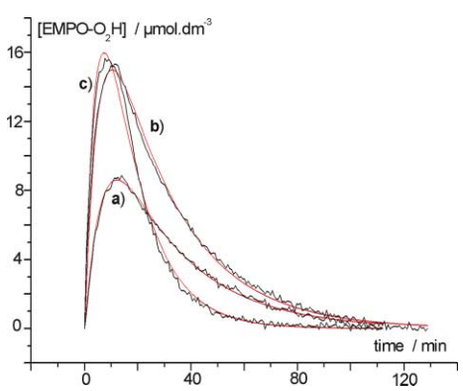

Fig. 3 Experimental (black) and calculated (red) kinetic curves indicating the time-dependent changes in the superoxide/EMPO spin adduct concentration [EMPO–O_2H]. EMPO–O_2H was produced at pH 7.2 by generating superoxide in the presence of: a) 0.01 mol dm^{-3} EMPO, b) 0.03 mol dm^{-3} EMPO, and c) 0.2 mol dm^{-3} EMPO. Calculated curves, obtained from eqns. (5)–(8), led to the following parameters: second-order rate constant for the trapping reaction, k_T = 10.9 dm^3 mol^{-1} s^{-1}; first-order rate constant for the adduct decay reaction, a) $k_D = 0.6\ 10^{-3}\ s^{-1}$, b) $k_D = 0.65\ 10^{-3}\ s^{-1}$, c) $k_D = 1.25\ 10^{-3}\ s^{-1}$.

curves jointly yielded the results reported in Table 1 for the rate constants k_T, and k_D. The corresponding simulated curves have been represented in Fig. 3 (red lines). The good fit between experimental and calculated curves confirms the validity of the kinetic model proposed. In addition, the low standard deviation in the parameters calculated (see Table 1) shows that our kinetic approach permitted the evaluation of accurate rate constants for the spin trapping of superoxide. Application of this technique to nitrones **2**–**6** led to the rate constant values listed in Table 1. As mention earlier, these k_T values are pH dependent apparent rate constants, which include the contribution of both $O_2^{-\bullet}$ and $HO_2^{\bullet}$ trapping.

With the exception of EMPO, the values obtained in this work for the apparent first-order rate constant k_D for the decay reaction of superoxide spin adducts (see Table 1) were consistent with those previously published,[4–6,8a,9] which corroborates the validity of our kinetic approach. As for EMPO (0.05 mol dm^{-3}), a k_D value of 2.4×10^{-3} s^{-1} has been reported in literature (0.05 mol dm^{-3} EMPO pH 7),[9a] which is significantly higher than that given in Table 1. Since we were not able to find an explanation for this discrepancy, we studied the decay of the adduct EMPO–O_2H apart from the spin trapping reaction, according to a method described previously.[4–6] In a parallel experiment performed at pH 7.2, superoxide was first produced in the presence of EMPO (0.05 mol dm^{-3}) using the X/XO generator, and the adduct formation was stopped by adding SOD (300 units cm^{-3}) 3 min after the reaction had begun. An EPR spectrum was then recorded over 40 min, in order to observe the adduct decrease in a single spectrum, and simulated with the computer program of Rockenbauer and Korecz.[7] The decay rate constant k_D calculated under these conditions was 0.6×10^{-3} s^{-1}, that is to say very close to the value given in Table 1. Consequently, we concluded that the half-life previously evaluated by Olive *et al.*[9a] for EMPO–O_2H was underestimated. As can be seen from Table 1, k_D was found dependent upon the concentration of the spin trap, the adduct decay being faster at higher nitrone concentration. This also appears clearly on Fig. 3, which shows that the maximum amount of EMPO–O_2H formed from 0.03 mol dm^{-3} EMPO (trace b) or from 0.2 mol dm^{-3} EMPO (trace c) are almost equal. This confirms a previous observation made in a study of the decay kinetics of DEPMPO–O_2H.[8a] We thus noticed that the adduct signal disappeared more rapidly when superoxide was generated in the presence of 0.2 mol dm^{-3} than in the presence of 0.1 mol dm^{-3}. This effect of the nitrone concentration on the amplitude of the DEPMPO–O_2H EPR signal was similarly observed by Roubaud *et al.*[18] The reason for this behaviour is still unclear and would certainly warrant a more thorough study. However, this should be taken into consideration when various nitrones are compared as regards the stability of their superoxide spin adducts, as well as in the aim of determining the optimum nitrone concentration for detecting superoxide.

It follows from Table 1 that cyclic nitrones trap superoxide more quickly than linear nitrones. When it comes to spin trapping efficiency, only TN **4**, which bears three nitrone functions, can be compared to **1**–**3**. This agrees with observations made by other researchers who found that the spin traps *N*-(1-oxidopyridin-1-ium-4-yl)methylidene]ethylamine *N*-oxide (4-PyOBN) and *N*-*tert*-butyl-benzylideneamine *N*-oxide (PBN) were much slower than DMPO at trapping superoxide.[11a,12a] An hypothesis that could justify the higher rate of trapping by cyclic nitrones could be the steric decompression in the five-membered ring associated to the change from a trigonal to a tetrahedral carbon, resulting from the trapping reaction. On the other hand, the same reaction diminishes the conjugation in the π-system of linear nitrones. In the case of nitrones **5** and **6**, the very low k_T value, eventually associated to a poor water-solubility, should be regarded as a serious drawback, which notably led us to modify our experimental procedure, as explained in the Experimental section. The data summarised in Table 1 also indicate that other effects can influence the spin trapping efficiency. Comparing the results obtained with EMPO **1**, DEPMPO **2** and DMPO **3** shows that the trapping rate is increased when an electron withdrawing group is attached to the 5-C position. This effect is even more marked if

Table 1 Rate constants for the spin trapping of superoxide by nitrones (k_T) and for the decay of nitrone/superoxide spin adducts (k_D) at pH 7.2

Nitrone	k_T/dm^3 mol^{-1} s^{-1}	Nitrone concentration/mol dm^{-3}	k_D/10^{-3} s^{-1}
EMPO **1**	10.9 ± 0.1	0.2	1.25 ± 0.04
		0.03	0.65 ± 0.04
		0.01	0.6 ± 0.04
DEPMPO **2**	3.95 ± 0.08	0.2	1.21 ± 0.05
		0.1	1.13 ± 0.05
		0.01	0.91 ± 0.05
DMPO **3**	2.0 ± 0.2	0.125	9.0 ± 0.8
		0.04	8.2 ± 0.8
		0.02	7.9 ± 0.8
TN **4**	8.9 ± 0.3	0.143	2.7 ± 0.1
		0.072	2.6 ± 0.1
		0.005	1.9 ± 0.1
EPPN **5**	0.02 ± 0.001	0.05	2.4 ± 0.1
		0.02	2.1 ± 0.1
EPPyON **6**	0.33 ± 0.01	0.08	6.9 ± 0.14
		0.05	4.8 ± 0.14

Table 2 Values previously published for the rate constant (k_T) of superoxide spin trapping with EMPO **1**, DEPMPO **2** and DMPO **3**

Nitrone	k_T/mol dm^{-3} s^{-1}	Competitive reaction	Ref.
EMPO **1**	74.5[a]	cytochrome c reduction	15
DEPMPO **2**	58[a]	SOD-dismutation	10
	0.53[b]	spontaneous dismutation	16
DMPO **3**	50[a]	DEPMPO-trapping	10
	2.4[a]	spontaneous dismutation	16

[a] pH 7. [b] pH 7.4.

we take into account the symmetry of these molecules. Actually, only the formation of the major diastereoisomer of the adduct was considered to evaluate k_T for **2**, while addition of superoxide on both sides of the five-membered ring of **3** yields the same adduct. According to recent results published by Tsai *et al.*,[15] the EPR signal recorded in the case of EMPO–O_2H corresponded to the addition of two diastereoisomers. This could partly explain the difference between DEPMPO **2** (k_T = 3.95 mol dm^{-3} s^{-1}, only the major diastereoisomer was considered) and EMPO **1** (k_T = 10.9 mol dm^{-3} s^{-1}, both diastereoisomers intervened).

As can be seen from Table 2, k_T values obtained in this work are globally much different than those recently published for EMPO **1**, DEPMPO **2** and DMPO **3**.[10,15,16] As mentioned earlier, the uncertainty associated with the assumed value of the rate constant for the reaction of superoxide with ferricytochrome c could explain why Villamena and Zweier[10] or Tsai et *al.*[15] obtained much higher k_T values than we did. The method used by Keszler *et al.*[16] seems to be closer to ours, since it also involves a direct competition with the superoxide spontaneous dismutation and a SVD procedure to achieve the kinetics curves. This is probably the reason why our results do not greatly differ from theirs. However, their kinetic treatment also necessitates the determination of superoxide production rate, by cytochrome c reduction. Therefore, our method is to date the only one yielding results which are completely free from errors connected to the use of cytochrome c reduction.

Whatever the nitrone considered, the low values determined for k_T indicate that the reaction of superoxide with nitrones is much slower than with other molecules commonly used to detect superoxide, such as ferricytochrome c.[17b,19,20] It means that high spin trap concentrations are required to trap out all the superoxide produced in a given medium before it decomposes *via* spontaneous dismutation. This should be regarded as a serious drawback of the spin trapping technique in quantitative measurements of superoxide, since it may result in an underestimation of the amount of this radical.

Conclusion

Our kinetic approach allowed an easy determination of rate constants for the superoxide/hydroperoxyl radical in buffered media. When compared to the use of competitive superoxide scavengers, this method presents the following advantages: 1) it requires less experimental work; 2) the medium does not contain a scavenger that could initiate side reactions; 3) errors due to either the determination of initial rates or the use of cytochrome c reduction are avoided; 4) neither the adduct decay reaction nor the dismutation of superoxide are neglected. Our results clearly show that, generally speaking, nitrones of the pyrrolidinic series are faster at trapping superoxide. Considering both the spin trapping rate and the spin adduct stability, EMPO **1** is obviously the most efficient nitrone for superoxide detection. However, even in this case, the superoxide trapping is quite slow. In addition, considering that spin adducts are readily reduced into EPR-silent hydroxylamines by a number of biochemical anti-oxidants, the question arises to know whether the EPR/spin trapping method could permit to quantify the amount of superoxide generated in biological systems or not. This crucial point has already been raised by other researchers who have compared for example the EPR spin trapping and the cytochrome c reduction techniques,[19] and perhaps the solution could be to cross different methods to obtain reliable results.[21] Despite the low rate constant for the reaction of superoxide with the spin traps tested, nitrones are still efficient superoxide detectors for qualitative study, and we believe that the development of their biological applications still necessitates the elaboration of new molecules with better spin trapping capacities.

Experimental

Materials

The nitrones EMPO **1**,[22] DEPMPO **2**,[13b] TN **4**,[5] EPPN **5**,[4] and EPPyON **6**,[6] were synthesised, purified, and identified in our laboratory according to procedures described previously. DMPO **3** was obtained from Sigma-Aldrich Chemical Co. and purified by fractional vacuum distillation before use. Diethylenetriaminepentacetic acid (DTPA), 3-carboxy-2,2,5,5-tetramethylpyrrolidin-1-oxyl (3CP), and xanthine were purchased from Sigma-Aldrich Chemical Co. Xanthine oxidase was obtained from Boehringer Mannheim Biochemica Co. Aqueous media were prepared from tri-distilled water. Buffer solutions were stirred gently for six hours in the presence of a chelating iminodiacetic acid resin (40 g dm^{-3}, Sigma-Aldrich Chemicals Co.) in order to remove trace metal impurities.

Deconvolutions based on singular value decomposition (SVD) and the pseudo-inverse

Though singular value decomposition (SVD) is a method deeply rooted in linear algebra, we will only describe very superficially its application to the deconvolution of EPR spectra evolving with time.[23] Those who are more interested in the SVD theory and its applications could refer for example to the paper written by Hendler and Shrager.[24]

When a digitised EPR signal is recorded as a function of time, the data set collected constitutes a matrix $\boldsymbol{A}$ in which each of the n columns represents a spectrum, and each of the m rows represents the kinetic evolution of a single point of the spectrum. Thus, the two dimensions of $\boldsymbol{A}$ correspond to two spaces of the phenomenon considered: the magnetic field in the columns, and the time in the rows. The SVD procedure permits to separate these two spaces into two individual matrices, *i.e.* $\boldsymbol{U}$ and $\boldsymbol{V}$ for the magnetic fields and the time, respectively, as shown in the following factorisation:

$$\boldsymbol{A} = \boldsymbol{U}\boldsymbol{S}\boldsymbol{V}^{\mathrm{T}}$$

$\boldsymbol{U}$ is of the same size as $\boldsymbol{A}$ (n columns, m rows). $\boldsymbol{V}$ is square and of dimension n. The SVD procedure produces a third matrix, called $\boldsymbol{S}$, which is square, diagonal, and of dimension n. Its diagonal elements are "singular values", and correspond to the weights of the columns of $\boldsymbol{U}$ and $\boldsymbol{V}$ in $\boldsymbol{A}$.

Application to noise-filtering. Examination of $\boldsymbol{S}$ shows that only a few of its diagonal elements are significantly different from zero. These non-zero singular values correspond to principal components of the EPR signal, while the other diagonal elements correspond to noise. Replacing these near-nil elements in $\boldsymbol{S}$ by zero yields a matrix $\boldsymbol{S}'$, and then a matrix $\boldsymbol{A}'$:

$$\boldsymbol{A}' = \boldsymbol{U}\boldsymbol{S}'\boldsymbol{V}^{\mathrm{T}}$$

All the spectral and temporal information contained in $\boldsymbol{A}$ is still present in $\boldsymbol{A}'$. In other words, the matrix $\boldsymbol{A}'$ leads to an EPR spectrum identical to that given by $\boldsymbol{A}$, but with an increased signal-to-noise ratio. The major advantage of the SVD procedure lies in the retention of kinetic information.

Achievement of kinetic curves by the pseudo-inverse method. The matrix $\boldsymbol{A}'$, in which the noise has been reduced, corresponds to the mixture of EPR spectra of several paramagnetic species which concentrations evolve with time. $\boldsymbol{A}'$ can be written as follows:

$$\boldsymbol{A}' = \boldsymbol{D}\boldsymbol{F}^{\mathrm{T}}$$

Each column of the matrix $\boldsymbol{D}$ contains the EPR spectrum of one component of the mixture, while each corresponding column of the matrix $\boldsymbol{F}$ represents the kinetic evolution of this single component. $\boldsymbol{D}$ also contains a column of 1, representing the background. Let us designate $\boldsymbol{D}^{+}$ the pseudo-inverse of $\boldsymbol{D}$:

$$\boldsymbol{D}^{+} = [\boldsymbol{D}^{\mathrm{T}}\boldsymbol{D}]^{-1}\boldsymbol{D}^{\mathrm{T}}$$

If the experimental or calculated EPR spectra making up $\boldsymbol{D}$ are known, $\boldsymbol{D}^{+}$ can be easily calculated from $\boldsymbol{D}$. Then, $\boldsymbol{F}^{\mathrm{T}}$ can be obtained as follows:

$$\boldsymbol{F}^{\mathrm{T}} = \boldsymbol{D}^{+}\boldsymbol{A}'$$

$\boldsymbol{F}$, which contains the kinetic information, indicates how the spectral components of $\boldsymbol{D}$ have to be linearly combined to give A′. This procedure thus permits the achievement of kinetic curves describing the evolution of each spectral components of $\boldsymbol{A}'$. These calculations were achieved with a home-made computer program written in FORTRAN, using subroutines given in Numerical Recipes.[25]

Achievement of experimental kinetic curves

EPR measurements were carried out at 20 °C in capillary tubes on a Bruker EMX spectrometer operating at X-band with 100 kHz modulation frequency. All the experiments were performed in 0.1 mol dm^{-3} phosphate buffers at pH 7.2. The xanthine/xanthine oxidase (X/XO) superoxide generator was used. In a standard experiment, the medium contained a nitrone (concentration ranging from 0.005 to 0.2 mol dm^{-3}), 3 mmol dm^{-3} DTPA, 1.6 mmol dm^{-3} xanthine, 3CP (0.54–1.08 μmol dm^{-3}), used as internal standard, and 0.4 units cm^{-3} xanthine oxidase. Air was bubbled into the medium for one min. before addition of xanthine oxidase. A part of the EPR signal showing at least one line of the superoxide adduct (N–O_2H) spectrum and one line of 3CP was then recorded every 42 s for at least two hours. This stable aminoxyl radical was chosen as internal standard because its concentration was found to be constant during our experiments. General instruments settings were as follows: non saturating microwave power, 20 mW; modulation amplitude, from 0.1 to 0.18 mT; receiver gain, from 2×10^5 to 2×10^6; time constant, 164 ms; scan time, 21 s; scan width, from 1.5 to 6 mT; 2 scans. According to this procedure, at least 240 spectra were recorded for each experiment. Noise was then reduced using the SVD procedure. Then, the spectrum recorded at a given time was considered separately. Its simulation led to : 1) the proportions, and thus the concentrations, of 3-CP and of N–O_2H; 2) the calculated spectra of 3-CP and of N–O_2H; 3) the proportions and the spectra of other species eventually present in the medium. The calculated spectra obtained permit the elaboration of the matrix $\boldsymbol{D}$, described earlier. The deconvolution method using the pseudo-inverse was then applied, thereby yielding the kinetic curves. Three experimental curves indicating the variation of the N–O_2H concentration with time were thus obtained for each nitrone at pH 7.2.

Considering that compounds **5** and **6** react particularly slowly with superoxide, the amount of nitrone necessary to trap out all the superoxide produced would be much too high in these cases. In addition, EPPN **5** is poorly water soluble. This led us to modify the experimental procedure as follows. The recording of the kinetic curve at the highest nitrone concentration, whose shape does not depend on the rate constants k_{T} and k_{dis}, was achieved using 200 mmol dm^{-3} DEPMPO instead of nitrones **5** and **6**. The curves at lower nitrone concentrations were obtained with compounds **5** or **6** themselves. For each nitrone considered, the three curves were then fitted simultaneously, which permitted us to determine k_{T}.

Determination of kinetic parameters

Computer modelling of the kinetic curves obtained was achieved using the home-made program KALIDAPHNIS. For each nitrone considered in this study, the program permits one to take into account simultaneously two, three or four experimental curves recorded at various nitrone concentrations. According to the model described by the rate equations (5)–(8), the variation of the spin adduct concentration with time depends on the initial concentrations of X, of superoxide, of nitrone, and of superoxide adduct, and on the rate constants k_{X}, k_{T}, k_{dis} and k_{D}. The nitrone initial concentration is an experimental parameter, while the initial concentrations of superoxide and of adduct are equal to zero. The value of the apparent rate constant for the dismutation of superoxide, k_{dis}, which can be calculated at various pH according to the formula of Behar *et al.*,[17a] is 4.03×10^5 dm^3 mol^{-1} s^{-1} at pH 7.2. The standard least-squares method is then applied to fit the experimental curves, yielding the kinetic parameters X_{i}, k_{X}, k_{T} and k_{D}, and the standard deviation of the calculated parameters.

It is important to specify here that the values obtained for the concentration [X] and for the rate constant k_X have no real meaning. These two parameters only come up as an empirical modelling of the superoxide source, and this is the reason why they are not given in this work. In particular, they may vary with the solutions of either xanthine or xanthine oxidase used. Therefore, it is of crucial importance to perform the three experiments at various concentrations with exactly the same superoxide generating system.

Kinetics of EMPO–O_2H decay

The X/XO system described above was used to produce superoxide in the presence of 0.05 mol dm^{-3} EMPO. Superoxide dismutase (SOD, 300 units cm^{-3}) was added to the medium 3 min after the reaction had begun. The medium was then transferred into an EPR capillary tube and the signal was recorded over 40 min in order to observe the adduct decay in a single spectrum. This spectrum was simulated by the computer program of Rockenbauer and Korecz[7] which allowed calculation of the rate constant k_D for the first-order decay of the adduct EMPO–O_2H.

References

1 (*a*) B. Halliwell and J. M. C. Gutteridge, in *Free Radicals in Biology and Medicine*, 2nd edn., Clarendon Press, Oxford, 1989; (*b*) M. Martinez-Cayelya, *Biochimie*, 1995, **77**, 147–161; (*c*) I. Fridovich, *J. Exp. Biol*, 1998, **201**, 1203–1209.

2 (*a*) C. Mottley and R. P. Mason, in *Biological Magnetic Resonance*, L. J. Berliner and J. Reuben (eds), Plenum Press,New-York, 1989, vol. 8, pp. 489–456; (*b*) M. J. Davies and G. S. Timmins, in *Biomedical Applications of Spectroscopy*, R. J. H. Clark and E. R. Hester, (eds), Wiley, Chichester, 1996; pp. 217–266; (*c*) S. Pou, H. J. Halpern, P. Tsai and G. M. Rosen, *Acc. Chem. Res.*, 1999, **32**, 155–161; (*d*) G. M. Rosen, E. Finkelstein and E. J. Rauckman, *Arch. Biochem. Biophys.*, 1982, **215**, 367–378; (*e*) G. M. Rosen and E. Finkelstein, *Free Radical Biol. Med.*, 1985, **4**, 345–375; (*f*) L. J. Berliner and H. Fujii, in *Biological Magnetic Resonance*, L. J. Berliner and J. Reuben (eds), Plenum, New York, 1992, vol. 11, pp. 307–319; (*g*) P. Tordo, *Electron Paramagn. Reson.*, 1998, **16**, 116–144.

3 G. R. Buettner and L. W. Oberley, *Biochem. Biophys. Res. Commun.*, 1978, **83**, 69–74.

4 V. Roubaud, R. Lauricella, J. C. Bouteiller and B. Tuccio, *Arch. Biochem. Biophys.*, 2002, **397**, 51–56.

5 V. Roubaud, H. Dozol, C. Rizzi, R. Lauricella, J. C. Bouteiller and B. Tuccio, *J. Chem. Soc., Perkin Trans. 2*, 2002, 958–964.

6 A. Allouch, V. Roubaud, R. Lauricella, J. C. Bouteiller and B. Tuccio, *Org. Biomol. Chem.*, 2003, **1**, 593–598.

7 A. Rockenbauer and L. Korecz, *Appl. Magn. Reson.*, 1996, **10**, 29–43.

8 (*a*) B. Tuccio, R. Lauricella, C. Frejaville, J. C. Bouteiller and P. Tordo, *J. Chem. Soc., Perkin Trans. 2*, 1995, 295–298; (*b*) V. Roubaud, R. Lauricella, B. Tuccio, J. C. Bouteiller and P. Tordo, *Res. Chem. Intermed.*, 1996, **22**, 405–416.

9 (*a*) G. Olive, A. Mercier, F. Le Moigne, A. Rockenbauer and P. Tordo, *Free Radical Biol. Med.*, 2000, **28**, 403–408; (*b*) H. Zhang, J. Joseph, J. Vasquez-Vivar, H. Karoui, C. Nzanzumuhire, P. Martasek, P. Tordo and B. Kalyanaraman, *FEBS Lett.*, 2000, **473**, 58–62; (*c*) H. Zhao, J. Joseph, H. Zhang, H. Karoui and B. Kalyanaraman, *Free Radical Biol. Med.*, 2001, **31**, 599–606.

10 F. A. Villamena and J. L. Zweier, *J. Chem. Soc., Perkin Trans. 2*, 2002, 1340–1344.

11 (*a*) E. Finkelstein, G. M. Rosen, E. J. Rauckman and J. Paxton, *Mol. Pharmacol.*, 1979, **16**, 676–685; (*b*) E. Finkelstein, G. M. Rosen and E. J. Rauckman, *Arch. Biochem. Biophys.*, 1980, **200**, 1–16; (*c*) E. Finkelstein, G. M. Rosen and E. J. Rauckman, *J. Am. Chem. Soc.*, 1980, **102**, 4994–4999; (*d*) G. M. Rosen, P. Tsai, J. Weaver, S. Porasuphatana, L. J. Roman, A. A. Starkov, G. Fiskum and S. Pou, *J. Biol. Chem.*, 2002, **227**, 40275–40280.

12 (*a*) N. Gotoh and E. Niki, *Chem. Lett.*, 1990, 1475–1478; (*b*) K. Mitsuta, M. Hiramatsu, H. Ohya-Nishiguchi, H. Kamada and K. Fujii, *Bull. Chem. Soc. Jpn.*, 1994, **67**, 529–538; (*c*) I. Yamazaki, L. H. Piette and T. Grover, *J. Biol. Chem.*, 1990, **265**, 652–659; (*d*) R. G. Gasanov and R. K. Freidlina, *Russ. Chem. Rev.*, 1987, **56**, 264–274.

13 (*a*) C. Frejaville, H. Karoui, B. Tuccio, F. Le Moigne, M. Culcasi, S. Pietri, R. Lauricella and P. Tordo, *J. Chem. Soc., Chem. Commun.*, 1994, 1793–1794; (*b*) C. Frejaville, H. Karoui, B. Tuccio, F. Le Moigne, M. Culcasi, S. Pietri, R. Lauricella and P. Tordo, *J. Med. Chem.*, 1995, **38**, 258–265.

14 (*a*) M. G. Simic, I. A. Taub, J. Tocci and P. A. Hurwitz, *Biochem. Biophys. Res. Commun.*, 1975, **62**, 161–167; (*b*) J. Butler, G. G. Jayson and A. J. Swallow, *Biochim. Biophys. Acta*, 1975, **408**, 215–222; (*c*) W. H. Koppenol, K. J. H. Van Buuren, J. Butler and R. Braams, *Biochim. Biophys. Acta*, 1976, **449**, 157–168; (*d*) Y. Kotake, L. A. Reinke, T. Tanigawa and H. Koshida, *Free Radical Biol. Med.*, 1994, **17**, 215–223.

15 P. Tsai, K. Ichikawa, C. Mailer, S. Pou, H. J. Halpern, B. H. Robinson, R. Nielsen and G. Rosen, *J. Org. Chem.*, 2003, **68**, 7811–7817.

16 A. Keszler, B. Kalyanaraman and N. Hogg, *Free Radical Biol. Med.*, 2003, **35**, 1149–1157.

17 (*a*) D. Behar, G. Czapski, J. Rabani, L. M. Dorfman and H. A. Schwarz, *J. Phys. Chem.*, 1970, **74**, 3209–3213; (*b*) M. Faraggi and C. Houée-Levin, *J. Chim. Phys.*, 1999, **96**, 71–84.

18 V. Roubaud, S. Sankarapandi, P. Kuppusamy, P. Tordo and J. Zweier, *Anal. Biochem.*, 1997, **247**, 404–411.

19 (*a*) J. M. McCord and I. Fridovich, *J. Biol. Chem.*, 1968, **243**, 5753–5760; (*b*) H. J. Forman and I. Fridovich, *Arch. Biochem. Biophys.*, 1973, **158**, 396–400; (*c*) W. Bors, M. Seran, E. Lengfelder, C. Michel, C. Fuchs and C. Frenzel, *Photochem. Photobiol.*, 1978, **28**, 629–638.

20 S. P. Sanders, S. J. Harrisson, P. Kuppusamy, J. T. Sylvester and J. L. Zweier, *Free Radical Biol. Med.*, 1994, **16**, 753–761.

21 L. J. Berliner, V. Khramtsov, H. Fujii and T. Clanton, *Free Radical Biol. Med.*, 2001, **30**, 489–499.

22 R. Bonnett, R. F. C. Brown, V. M. Clark, I. O. Sutherland and S. A. Todd, *J. Chem. Soc.*, 1959, 2094–2100.

23 O. Steinbock, B. Neumann, B. Cage, J. Saltiel, S. C. Müller and N. S. Dalal, *Anal. Chem.*, 1997, **69**, 3708–3713.

24 R. W. Hendler and R. I. Shrager, *J. Biochem. Biophys. Methods*, 1994, **28**, 1–33.

25 W. H. Press, S. A. Teukolsky, W. T. Vetterling and B. P. Flannery, in *Numerical Recipes in FORTRAN: the art of scientific computing*, 2nd edn., Cambridge University Press, Cambridge, 1992.